

ION BEAM CHARGE NEUTRALIZATION BY FERROELECTRIC DISCHARGE PLASMA *

A.D. Stepanov, E.P Gilson, L.R. Grisham, R.C. Davidson
 Princeton Plasma Physics Laboratory, Princeton, New Jersey, 08543, USA

Abstract

Space-charge forces limit the possible transverse compression of high perveance ion beams that are used in ion-beam-driven high energy density physics applications; the minimum radius to which a beam can be focused is an increasing function of perveance. The limit can be overcome if a plasma is introduced in the beam path between the focusing element and the target in order to neutralize the space charge of the beam. This concept has been implemented on the Neutralized Drift Compression eXperiment (NDCX) at LBNL using Ferroelectric Plasma Sources (FEPS). In experiments at PPPL, a perveance-dominated ion beam was propagated through a FEPS and the transverse beam phase space was measured with a slit-slit emittance scanner to characterize the effect of charge-neutralizing plasma on beam divergence.

INTRODUCTION

To reduce the divergence of high-perveance ion beams due to space charge, electrons can be introduced into the beam volume. In most experimental applications, electrons are produced by ion impact ionization of background gas and from secondary electron emission (SEE) from surfaces impacted by the beam. Electrons become confined the electrostatic potential well of the ions, reducing the magnitude of the potential well, which decreases until equilibrium is established between electron production and loss rates. For charge neutralization by ionization of background neutrals, this process typically takes $50 \mu\text{s}$.

For charge neutralization of pulsed ion beams with duration $< 100 \mu\text{s}$, a volume plasma can be introduced into the beam path to provide electrons. Ferroelectric Plasma Sources (FEPS) can produce volume plasmas with low electron temperatures, and have been used successfully on NDCX-I to neutralize the space charge of a converging high-perveance ion beam pulse. Herein, experiments on charge neutralization of a 32-42 keV Ar+ beam with a plasma produced in a ferroelectric discharge are presented.

FERROELECTRIC PLASMA SOURCES

Ferroelectric materials (FE), such as PZT and (BaTiO_3) are characterized by a high relative dielectric constant ($\epsilon_r > 1000$) and the presence of a spontaneous electric polarization. It was found that under the application of a fast-changing electric field, high electron current densities are emitted from the FE surface [1, 2], and plasma can

be produced. Plasma sources based on BaTiO_3 have been built for use on NDCX-I/II [3] for ion beam charge neutralization. The basic configuration of a ferroelectric plasma source (FEPS) is a slab of ferroelectric material placed between two flat electrodes, one of which is perforated. When a fast-rising voltage pulse ($\sim 5 \text{ kV}$) is applied between the electrodes, a plasma is formed at the side of the perforated electrode at points of juncture between metal, ceramic, and vacuum. In addition, gas desorption occurs during FEPS discharge, which most likely plays a role in plasma formation. The precise mechanism of operation of FEPS is still under investigation [4].

EXPERIMENTAL SETUP

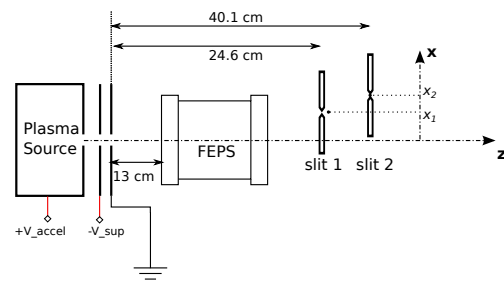


Figure 1: Diagram of the beamline used in the experiment. An Ar^+ beam, extracted from a plasma, propagates through a cylindrical FEPS. Downstream of the FEPS, the beam is intercepted by a two-slit emittance scanner which is used to measure the transverse current distribution of the beam.

The experiments were carried out on the Princeton Advanced Test Stand (PATS) at PPPL. Ar^+ ions are extracted from an RF-driven plasma and formed into a beam with a 3-electrode, accel-decel extraction system with gap length $d = 1.1 \text{ cm}$ and plasma aperture with radius $r_B = 1.5 \text{ mm}$. The plasma is generated in a multicusp RF source with an internal antenna [5], driven by a pulsed RF power supply. Ion current density up to 28 mA/cm^2 can be extracted. Accelerating potential V_{accel} (30-60 kV) is supplied by an HV pulser [6].

The ion beam exits the accelerator through a grounded aperture at $z = 0$. At $z = 13 \text{ cm}$, the beam enters a 10.1 cm long FEPS with an inner diameter of 7.62 cm. After the FEPS, the beam is intercepted by a slit-slit emittance scanner. The slits, located at $z_1 = 24.6 \text{ cm}$ and $z_2 = 40.1 \text{ cm}$, are 2.5" long, 0.1 mm wide, and oriented horizontally. The second slit, referred to as the slit-cup, has a Faraday cup (FC) with SEE suppressor grid mounted directly behind it

* This work is supported by US DOE contract DE-AC02-09CH11466

for measuring ion current. Both slits are mounted on linear motion feedthroughs and can be moved in the vertical direction. The feedthroughs are driven by stepper motors, which provide positioning accuracy better than 0.1 mil.

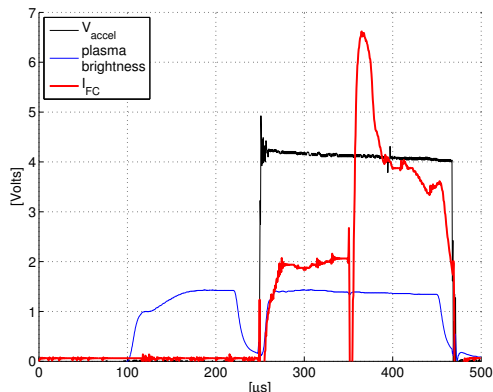


Figure 2: Waveforms of plasma density (blue trace), accelerating potential V_{accel} (black trace, 1 V = 10 kV), and FC current I_{FC} (red trace, 1 V = 1 μ A) measured with the slit-cup positioned on beam axis. $V_{accel} = 42$ kV and $I_B = 0.7$ mA. FEPS was triggered at $t = 350$ μ s. Plasma density is inferred from plasma light emission intensity.

The emittance scanner diagnostic provides y -integrated measurements of the transverse distribution $f(x, v_x, y, v_y)$. The first slit can be moved out of the way, so the beam is intercepted by the slit-cup only. Then, y -integrated transverse current density profiles $I_{FC}(x_2) = \int j(x_2, y) dy$ at $z = z_2 = 40.1$ cm can be obtained by recording I_{FC} for a range of slit-cup positions. If the beam is made to pass through both slits, then the current $I_{FC}(x_1, x_2)$ will be due to beam ions with $x = x_1$ and transverse angle $x' = (x_2 - x_1)/D$, where $D = z_2 - z_1 = 15.5$ cm is the z -distance between the slits. In this way, the y -integrated trace-space distribution $f(x, x')$ at $z = z_1 = 24.6$ cm can be measured.

In the experiment, ion beam pulses were generated every 2 seconds, with 200 μ s-long RF and V_{accel} pulses applied concurrently. Afterglow plasma from an earlier RF pulse (from $t = -180$ μ s to $t = -30$ μ s) was used as source of electrons to improve RF breakdown and plasma density rise-time. The FEPS was triggered 100 μ s after the start of beam pulse. Typical waveforms of $I_{FC}(t)$, $V_{accel}(t)$ and plasma density are shown in Fig. 2.

EXPERIMENTAL RESULTS

In general, the beam divergence was greatly reduced when the FEPS was triggered, as can be seen in Fig. 2, showing $I_{FC}(t)$ for the slit-cup positioned on the beam axis. The increase in current after the FEPS is triggered at $t = 350$ μ s, corresponds to the narrowing of the beam profile. $I_{FC}(t)$ reaches a maximum 15 μ s after the FEPS discharge. Data from slit-cup profile scans and trace-space scans is used to investigate the timing and duration of

charge neutralization and the minimum beam divergence that can be attained.

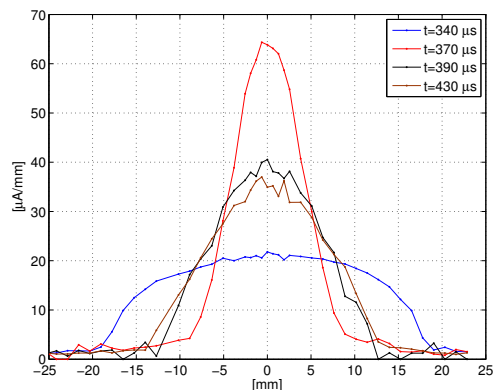


Figure 3: Transverse current density profiles $I_{FC}(x_2)$ taken with the slit cup at different times in the shot.

In the analysis, the effectiveness of neutralization is characterized by a decrease in beam divergence. For an ion beam extracted from a free plasma boundary, experimentally measured divergence is due several factors. The beam will expand due to space charge, characterized by generalized perveance $Q = (1/4\pi\epsilon_0)\sqrt{M/2eI_B/V_{accel}^{3/2}}$, and transverse emittance ϵ , due to finite temperature of plasma ions. These effects are included in the envelope equation for $r(z)$:

$$\frac{dr^2}{dz^2} = \frac{Q}{r} + \frac{\epsilon^2}{r^3} \quad (1)$$

Equation (1) can be solved numerically with initial conditions (r, r') at $z = 0$, which correspond to initial beam radius and divergence at the exit of the accelerator. In a plasma ion source, beam current and accelerating potential can be controlled independently, and the initial divergence of the beam depends on the perveance match. According to [7], the divergence angle $\omega = 0.29S(1 - 2.14Q/Q_0)$, where S is the aspect ratio of the extraction gap and Q_0 is the optimal perveance. The optimal divergence that was obtained experimentally in [7] was 1.2° , as measured by $1/e$ Gaussian half-width.

In order to compare experimental results to the envelope model, transverse current density profiles $I(x)$ are measured with the slit-cup for beam energies of 32, 38, and 42 kV, and beam currents from 0.4 to 0.8 mA. Time evolution of total current $I_B(t)$ and HWHM profile width $x_{HWHM}(t)$, calculated from profiles of $I(x)$, is shown in Fig. 4. $I_B(t)$ remains the same before and after the FEPS is triggered, except for the dip in at 350 μ s due to electrical noise from the FEPS HV pulse. The curve of $x_{HWHM}(t)$ shows that before neutralization, $x_{HWHM}(t)$ reaches steady state quickly. After the FEPS is triggered, $x_{HWHM}(t)$ decreases to a minimum at $t = 365$ μ s, and then increases but remains smaller than before neutralization. Transverse current density profiles at different times are plotted in Fig. 3.

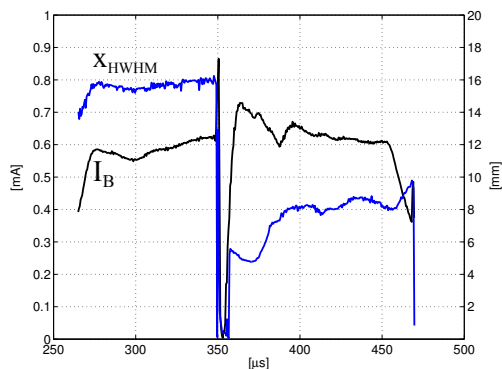


Figure 4: Time evolution of total beam current I_B (black trace) and x_{HWHM} (blue trace) computed from slit-cup profile data for $V_{accel} = 42$ kV, $I_B = 0.7$ mA

Beam divergence, characterized by half-width, half-max of profiles $I(x)$ is plotted as a function of Q in Fig. 5 before neutralization ($t = 340$ μ s, blue dots) and at optimal neutralization ($t = 365$ μ s, red dots). Beam radius $r_B(Q)$ calculated from the envelope equation with $r(z = 0) = 0.15$ cm and $r'(z = 0) = 0$ is shown for comparison. For the unneutralized case, x_{HWHM} monotonically increases with Q , consistent with space charge expansion. For the neutralized case, x_{HWHM} vs Q has the shape of a perveance curve with a minimum at $Q \simeq 2.9 \times 10^{-4}$, suggesting that beam divergence is due to perveance match in the accelerating gap. At optimum perveance, the 1/e Gaussian half-width divergence angle is equal to 0.87° .

This angular divergence is close to optimal divergence of 1.2° obtained in [7] with a DC ion beam neutralized by ionization of neutral gas. This suggests that observed divergence is due to initial divergence at the exit of the accelerator, and that the beam propagated with $Q_{eff} \simeq 0$ from the source to the diagnostic. This means that that electrons from the FEPS plasma filled the volume of the whole beam and the beam propagated ballistically. This is evident from measurements of the trace-space distribution $f(x, x')$ with the two slit method.

In order to visualise the shape of the beam ellipse in $x - x'$ trace-space, a transformation $x' \rightarrow x'_2$ was applied:

$$x'_2 = x_2 - \frac{D_2 + D_1}{D_1} x_1 = x_2 - 1.61 x_1 \quad (2)$$

Here, D_1 and D_2 are distances from the extractor to the first and second slits respectively. With this transformation, the horizontal line $x'_2 = 0$ corresponds to the two slits being positioned on line-of-sight to the extractor. In Fig. 6, results of trace-space measurements are shown, comparing an unneutralized beam with the beam during optimal neutralization, which occurs 15 μ s after the FEPS is triggered. The unneutralized beam has greater laminar divergence than lines-of-sight to the extractor, with the apparent source point located at $z = 3.6$ cm. This is consistent with space-charge expansion, when divergence angle r' increases with z . In the neutralized case, the beam trajectory

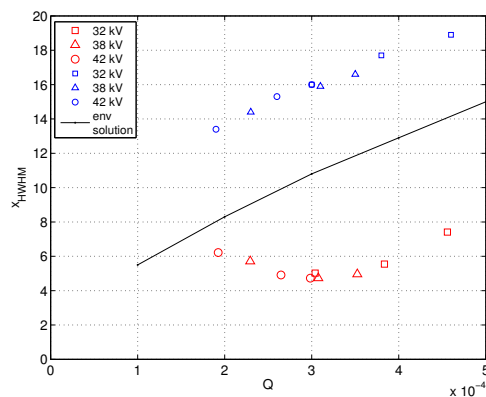


Figure 5: Profile widths characterized by x_{HWHM} versus generalized perveance Q for unneutralized (blue) and neutralized (red) cases at $z = 40.1$ cm. The solution to the envelope equation $r_B(Q)$ (black) is also plotted.

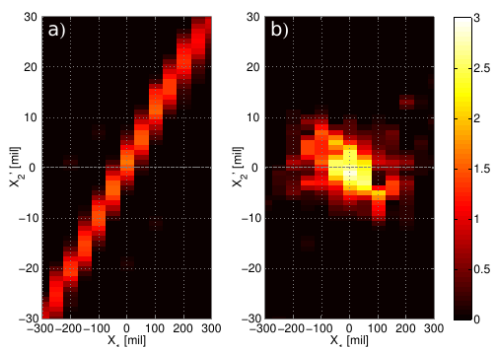


Figure 6: Trace-space data a) before neutralization ($t = 340$ μ s) and b) after neutralization ($t = 365$ μ s). The horizontal line $x'_2 = 0$ corresponds to straight ion trajectories from the extraction aperture of the ion beam to the diagnostic.

ries are more convergent than lines-of-sight to the extractor, with the apparent source point located at $z < 0$. This indicates that the ion beam was completely charge-neutralized by FEPS plasma.

REFERENCES

- [1] A. Dunaevsky et al, Journal of Applied Physics, 95:4621, 2004
- [2] G. Rosenman et al, Appl. Phys. Rev., 88:6109, 2000
- [3] E.P. Gilson, et al., Nuclear Instruments & Methods in Physics Research A (2013)
- [4] V.T. Gurovich, et al, Journal of Applied Physics 106 (2009) 053301.
- [5] G. Westenskow, et al. "Characterization of an RF-driven plasma ion source for Heavy Ion Fusion," PAC'03, pp.3300
- [6] M.J. Wilson, D. Goerz, R. Speer, and R. Moal. "Heavy Ion Fusion (HIF) Impulse Injector Design, Construction, and Checkout". LLNL Report UCRL-ID-130764,1998.
- [7] J.R. Coupland, et al, Review of Scientific Instruments, vol.44, no.9, pp.1258, 1973